Progress In Electromagnetics Research M, Vol. 22, 271–287, 2012

EMC ANALYSIS OF ANTENNA SYSTEM ON THE ELECTRICALLY LARGE PLATFORM USING PARALLEL MoM WITH HIGHER-ORDER BASIS FUNCTIONS

Y. Yan[1, *], Y. Zhang[1], C.-H. Liang[1], D. García-Doñoro[2], and H. Zhao[3]

[1]Science and Technology on Antenna and Microwave Laboratory, Xidian University, Xi'an, Shaanxi 710071, China

[2]Department of Signal Theory and Communications, University Carlos III of Madrid, Leganés 28911, Spain

[3]Department of Aerial Platform System, China Academy of Electronics and Information Technology, Beijing 100041, China

Abstract—Currently, more and more practical engineering applications place antenna system on the electrically large platform. This paper deals with the problem of antennas mounted on large platform from two aspects — radiation pattern and system electromagnetic compatibility (EMC). To achieve an accurate and effective computation, this paper applies method of moment (MoM) with Higher-order basis functions solver with large-scale parallel computation technique. And finally some real-life examples are presented to describe how to install antennas on the platform reasonably.

1. INTRODUCTION

Since high-tech weapon plays an important role in the modern warfare, the systematical integration characteristic becomes more and more significant in various weapon platforms and systems. Electronic countermeasure is a main form of the high-tech warfare, so the number of radio frequency devices used in detection, disturbing and confusion becomes larger and larger, and the amount and type of these antennas on a specific platform increase rapidly. So a platform with many antennas presents a challenge problem to the analysis of system's

Received 24 October 2011, Accepted 22 December 2011, Scheduled 3 January 2012

* Corresponding author: Ying Yan (yymqn1008@163.com).

EMC. A question of how to calculate the compatibility among different antenna systems has been proposed.

To solve this problem, one traditional and widely adopted method is the method of moments (MoM) [1, 2]. However, when the simulation frequency is high, the MoM method based on the Rao-Wilton-Glisson basis functions (RWGs) [3–6] produces a very large number of unknowns for electrically large structures. To reduce the number of unknowns and accelerate the computation, the Fast Multipole Method (FMM) [7] and Multi-level Fast Multipole Method (MLFMM) [8] are two feasible approaches. Although these techniques can achieve our goal in some extent, the problem of convergence will emerge when the model to be simulated is complex, which results in instability of the computational process. As another class of effective technique, hybrid methods of high and low frequencies are widely used to solve the EMC problems, such as MoM-UTD [9, 10], MoM-PO [11–14], etc. Usually, this kind of method divides the model into two parts: the MoM region (i.e., some specific structures such as the antennas on the platform) and the high frequency region (the platform with electrically large dimensions). Although this kind of method can effectively shorten the computational time and reduce the computational amount, the precision will be poor. If we have to analyze the problem accurately, this kind of method will not be suitable.

From what have been described above, we choose the MoM with higher-order basis functions [1, 16, 17]. In this method, higher-order polynomials over wires and quadrilateral plates are used as basis functions over larger subdomain patches so that this procedure can be approximately related to the use of entire domain basis functions [15]. Polynomial expansions for the basis functions over larger subdomains result in a good approximation of the current distributions over large surfaces using approximately 10 unknowns per wavelength squared of surface area. Therefore, the use of polynomial basis functions over larger patches sharply reduces the number of unknowns required to approximate the unknown solution, compared with the number of piecewise RWG basis functions. We use the direct solving method — LU decomposition to solve the obtained linear equation, thus there will not exist the problem of convergence. And the precision can be guaranteed since the solving process is the same as conventional MoM [2], except replacing the basis functions by Higher-order basis functions.

Moreover, a large-scale electromagnetic (EM) parallel computation solver is the optimum method [1, 18–20] to solve some electrically large EMC problems, which includes EMC analysis, antennas' layout and the integration of the platform and the antennas.

In this paper, the parallel MoM solver combined with the higher-order polynomial basis functions (HOBs) is employed on high-performance clusters to calculate the radiation pattern of antennas on the platform and to analyze EMC problem between them.

In the second section of this paper, the basic theory of higher-order basis function and the parallel scheme of MoM are presented, respectively, and then the computational platforms are described. Section 3.1 validates the accuracy of this paper's method through the comparison with the RWG (Rao-Wilton-Glisson) MoM [3–6] method's result, then some more numerical examples of EMC problem are described. Section 3.2 presents a real-life problem of some linear antennas distributed on a plane. Section 3.3 gives another example of three Yagi antennas and two patch antennas mounted on a MIG29 plane. Sections 4 and 5 give the conclusion and the acknowledgement, respectively.

2. BASIC THEORY

2.1. Higher-order Basis Functions

Flexible geometric modeling can be achieved by using truncated cones for wires and bilinear patches to characterize surfaces [1].

The surface current over a bilinear surface is decomposed into its p and s-components, as shown in Fig. 1(a). However, the p-current

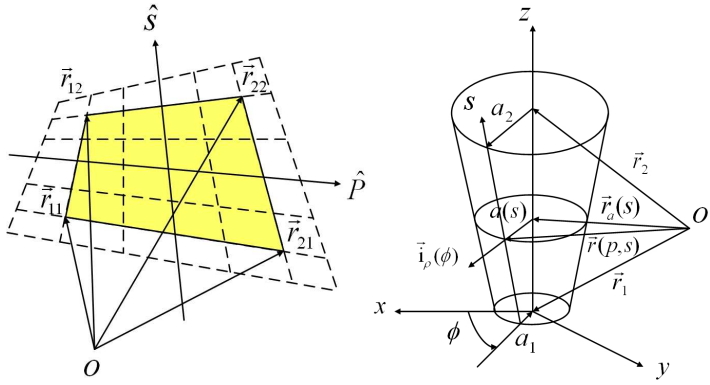

Figure 1. Geometric model: (a) A bilinear surface defined by four vertices; (b) A right-truncated cone defined by position vectors and radii of its beginning and end.

component can be treated as the s-current component defined over the same bilinear surface with an interchange of the p and s coordinates. The approximations for the s-components of the electric and magnetic currents over a bilinear surface are typically defined as

$$\vec{J}_s(p,s) = \sum_{i=0}^{N_p} \left[c_{i1}\vec{E}_i(p,s) + c_{i2}\vec{E}_i(p,-s) + \sum_{j=2}^{N_s} a_{ij}\vec{P}_{ij}(p,s) \right] \tag{1}$$

where $c_{i1},\ c_{i2},\ (i = 0, 1, \ldots, N_p)$ are defined as [1]

$$c_{i1} = \sum_{j=0}^{N_s} a_{ij}(-1)^j, \quad c_{i2} = \sum_{j=0}^{N_s} a_{ij} \tag{2}$$

The edge basis functions $\vec{E}_i(p,s)$ and the patch basis functions $\vec{P}_{ij}(p,s)$ $(i = 0, \ldots N_p, j = 2, \ldots, N_s)$ are expressed by (3) and (4) respectively

$$\vec{E}_i(p,s) = \frac{\vec{\alpha}_s}{|\vec{\alpha}_p \times \vec{\alpha}_s|} p^i N(s) \tag{3}$$

$$\vec{P}_{ij}(p,s) = \frac{\vec{\alpha}_s}{|\vec{\alpha}_p \times \vec{\alpha}_s|} p^i S_j(s) \tag{4}$$

where $\alpha_p,\ \alpha_s$ are the unitary vectors defined as

$$\vec{\alpha}_p = \frac{\partial \vec{r}(p,s)}{\partial p}, \quad \vec{\alpha}_s = \frac{\partial \vec{r}(p,s)}{\partial s} \tag{5}$$

Node basis function $N(s)$ and segment basis functions $S_i(s)$ $(i = 2, \ldots, N_s)$ are expressed as

$$N(s) = \frac{1-s}{2}, \quad S_i(s) = \begin{cases} s^i - 1, & i \text{ is even} \\ s^i - s, & i \text{ is odd} \end{cases} \tag{6}$$

The parametric equation of such an isoparametric element (i.e., bilinear surface) can be written in the following form as

$$\begin{aligned} &\vec{r}(p,s) = \vec{r}_{11}\tfrac{(1-p)(1-s)}{4} + \vec{r}_{12}\tfrac{(1-p)(1+s)}{4} + \vec{r}_{21}\tfrac{(1+p)(1-s)}{4} + \vec{r}_{22}\tfrac{(1+p)(1+s)}{4} \\ &-1 \le p \le 1, \quad -1 \le s \le 1 \end{aligned} \tag{7}$$

where $\vec{r}_{11},\ \vec{r}_{12},\ \vec{r}_{21},\ \vec{r}_{22}$ are the position vectors of its vertices, and the p and s are the local coordinates.

Generalized wires (i.e., wire that has a curvilinear axis and a variable radius) can be approximated by right-truncated cones. A right-truncated cone is determined by the position vectors, and the radii of its beginning and end are, respectively, as shown in Fig. 1(b).

Currents along wires are approximated by polynomials and can be written as

$$I(s) = I_1 N(s) + I_2 N(-s) + \sum_{i=2}^{N_s} a_i S_i(s), \quad -1 \le s \le 1 \tag{8}$$

where the node basis function, $N(s)$, and the segment basis functions, $S_i(s)$ $(i = 2, \ldots, N_s)$, are expressed as

$$N(s) = \frac{1-s}{2}, \quad S_i(s) = \begin{cases} s^i - 1, & i \text{ is even} \\ s^i - s, & i \text{ is odd} \end{cases} \tag{9}$$

Respectively, $a_i (i = 2, \ldots N_s)$ are the coefficients, and $I_1 = I(-1)$, $I_2 = I(1)$ are the values of the currents at the wire ends, respectively.

The parametric equation of the cone surface can be written as

$$\vec{r}_a(\phi, s) = \vec{r}_a(s) + a(s)\vec{i}_\rho(\phi), \quad -1 \le s \le 1, -\pi \le \phi \le \pi \tag{10}$$

$$\vec{r}_a(s) = \vec{r}_1 + (s - s_1)\frac{\vec{r}_2 - \vec{r}_1}{s_2 - s_1}, \quad s_1 \le s \le s_2 \tag{11}$$

$$a(s) = a_1 + (s - s_1)\frac{a_2 - a_1}{s_2 - s_1}, \quad s_1 \le s \le s_2 \tag{12}$$

As illustrated in Fig. 1(b), s is the local coordinate along a cone generatrix (in mathematics, the surface traced by a moving straight line (the generatrix) that always passes through a fixed point (the vertex). In Fig. 1(b), line S is the generatrix of the cone), ϕ is the circumferential angle, measured from the x-axis, and $\vec{i}_\rho(\phi)$ is the radial unit vector, perpendicular to the cone axis.

2.2. Parallel Scheme of MoM

The parallelization of the MoM solution involves two steps. The first step is the matrix filling and the second step is the solution of the matrix equation. Both of these must be handled efficiently. Furthermore, efficient parallel matrix filling for MoM with Higher-order basis introduces new challenges and is quite different from the procedure used in a MoM formulation using the traditional subdomain basis functions, e.g., RWGs [19]. To parallelize the solution of the large dense matrix in a MoM problem, typically one needs to divide the matrix between processes in such a way that two important conditions are fulfilled: each process should store approximately the same amount of data, and the computational load should be equally distributed among the processes that run on different nodes.

The parallel LU decomposition based on the ScaLAPACK [1] library package is employed as the solver and the block storage scheme is designed accordingly. Assume that the matrix **A** is a large dense matrix; it can be divided into smaller blocks and distributed to each process grid [1]. For explanation purposes, the MoM matrix equation is rewritten in a general form as

$$AX = B \tag{13}$$

where **A** denotes the complex dense matrix (i.e., impedance matrix Z of MoM), **X** is the unknown vector (i.e., coefficient of current I) to be determined and **B** denotes the given source vector (i.e., excitation V of MoM).

For example, we assume that the matrix **A** is divided into 6×6 blocks, which are distributed to 6 processes in a 2×3 process grid, as illustrated in Fig. 2(a). Fig. 2(b) shows to which process the blocks of **A** are distributed using the ScaLAPACK's distribution methodology [1].

In Fig. 2(a), the outermost numbers denote the row and column indices of the process coordinates. The top and bottom numbers in any block of Fig. 2(b) denote the process rank and the process coordinate of a certain process respectively, corresponding to the block of the matrix shown in Fig. 2(a). By varying the dimensions of the blocks of A and those of the process grid, different mappings can be obtained. This

Process unit index

	0	1	2	0	1	2
0	11	12	13	14	15	16
1	21	22	23	24	25	26
0	31	32	33	34	35	36
1	41	42	43	44	45	46
0	51	52	53	54	55	56
1	61	62	63	64	65	66

(a)

0 (0,0)	2 (0,1)	4 (0,2)	0 (0,0)	2 (0,1)	4 (0,2)
1 (1,0)	3 (1,1)	5 (1,2)	1 (1,0)	3 (1,1)	5 (1,2)
0 (0,0)	2 (0,1)	4 (0,2)	0 (0,0)	2 (0,1)	4 (0,2)
1 (1,0)	3 (1,1)	5 (1,2)	1 (1,0)	3 (1,1)	5 (1,2)
0 (0,0)	2 (0,1)	4 (0,2)	0 (0,0)	2 (0,1)	4 (0,2)
1 (1,0)	3 (1,1)	5 (1,2)	1 (1,0)	3 (1,1)	5 (1,2)

(b)

Figure 2. Block-cyclic distribution of a matrix: (a) a matrix consisting of 6×6 blocks ; (b) rank and coordinates of each process owning the corresponding blocks in (a).

scheme can be referred to as a "block-cyclic" distribution procedure.

Note that the storage required for the vectors X and B is negligible compared with that of the large dense matrix A. Therefore, the entire vectors can be stored in each process.

Load balancing is critical to obtain an efficient operation of a parallel code. This parallel scheme of matrix filling is able to achieve the good load balancing. Little communication between processes is necessary during the matrix filling [1].

As we use the parallel LU decomposition solver, when the matrix filling is finished, the next step is to perform the LU decomposition. A recursive algorithm can be developed according to the LU decomposition, which computes one block of row and column at each step and uses them to update the trailing sub-matrix. The procedure starts by having the processes that hold portions of the column panel consisting all the blocks of this column collaborate within the rows of processes to the other columns. Due to the "block-cyclic" scheme presented above, the problem deflates as the algorithm proceeds, but the processes continue to participate instead of becoming idle.

After the entire matrix is decomposed, the solution of Eq. (13) involves two steps, a forward substitution and a backward substitution [1].

2.3. Formula of the Isolation

Isolation of antennas is an important index for electromagnetic compatibility (EMC) on various of platforms. For example, as illustrated in Fig. 3, antennas 1, 2 and the PEC convex surface can be equivalent to a network with two ports. Antenna 1 and antenna 2 are considered as these two ports. The isolation between port 1 and port 2 can be defined as: port 1 is connected to signal source, while port 2 connects a load, the ratio of the load's absorbing power P_L to the signal source's available power P_a.

$$IDL\ (\text{dB}) = 10\log\left(\left|{}^{P_L}\!/_{P_a}\right|\right) \tag{14}$$

it can also be derived into

$$IDL(\text{dB}) = -10\log\left(\frac{|S_{21}|^2}{(1-|S_{11}|^2)(1-|S_{22}|^2)}\right) \tag{15}$$

To compute the isolation parameters between these two ports, we first calculate the S parameters of S_{11}, S_{12}, S_{21}, S_{22} [2], and then substitute them into Eq. (15).

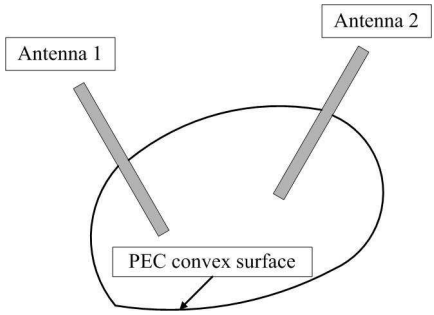

Figure 3. Two line antennas on a PEC convex surface.

2.4. Description of the Computational Platforms

The computer platforms have been used to perform the calculation are listed as follows:

1) Personal Computer: Quad core Intel I5 processor (2.67 GHz) with 4 GB RAM and 500 GB of hard disk.

2) Shanghai Supercomputer Center (SSC) [21]: The 37 nodes from Magic-cube Machine with a total of 592 AMD CPU cores (1.9 GHz per CPU and 4 cores on each CPU): 16 CPU cores on each node and 4 GB RAM per core, and a total of RAM approximately equal to 2.3 TB. No hard disk storage is available for computation. Infiniband is used for the network interconnection.

3. NUMERICAL EXAMPLES AND DISCUSSION

3.1. Algorithm Validation

To validate the accuracy of the proposed parallel Higher-order basis MoM methodology, two "Case Studies" are illustrated: (1) a linear antenna mounted on the top of the truncated cone to calculate its radiation pattern; (2) two linear antennas mounted at the different location of the truncated cone to calculate their isolations in a frequency range.

3.1.1. Case Study 1

The first "Case Study" is a wire antenna mounted on the top of a truncated cone.

The cone is end-capped and oriented along the z-axis and centered in the plane $z = 0$. The height is 200 mm, the major diameter 200 mm, and the minor one 100 mm.

A wire antenna along the positive z-axis is distributed on the top surface of the truncated cone and connected to this surface. A unit voltage source on the junction of the cone and the antenna is used to be the feeder.

The model is simulated at 7 GHz, and the radiation pattern on XOZ plane has been calculated to compare with the result from RWG MoM method [3–6]. Since the cone model is symmetrical on XOY plane, the radiation patterns on XOZ and YOZ planes are the same, and the result on XOY plane is non-directional. Thus, the result on XOZ plane is chosen as the comparison data.

In this simulation, the elevation angle (θ) is taken from the positive z-axis and azimuth angle (ϕ) from the positive x-axis. The first kind of computer platform described above is used to perform the calculation.

Figure 4 shows the model simulated and the results comparison between this paper's method and the RWG MoM method. There is a good agreement between the results obtained by these two methods.

3.1.2. Case Study 2

The second "Case Study" is two wire antennas mounted at different locations of the truncated cone. The cone has the same size as that in "Case Study 1". Two wire antennas are connected to the surface of the cone. The wire antennas' location is presented in Table 1. Moreover, the unit voltage source on the junction of the cone and the antenna is used to be each antenna's feeder.

The model is simulated at the frequency from 5 GHz to 7 GHz.

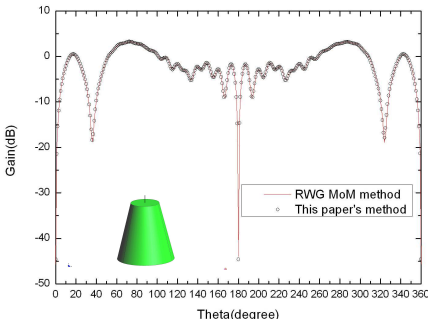

Figure 4. Radiation pattern of a wire antenna mounted on the truncated cone. Frequency: 7 GHz. Comparison with RWG MoM method.

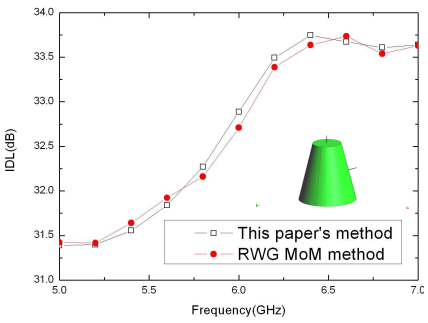

Figure 5. The isolation between the two antennas versus frequency.

Table 1. The coordinates of antenna 1 and 2 (unit: m).

	x	y	z
start point of antenna 1	0	0	0.1
end point of antenna 1	0	0	0.125
start point of antenna 2	0	0.075	0
end point of antenna 2	0	0.09925	0.00606

The isolation between antennas 1 and 2 has been calculated to compare with the result from RWG MoM method [3–6], as shown in Fig. 5.

From Fig. 5, it can be found that the results of this paper's method and RWG MoM agree well.

3.2. An Aircraft with Some Linear Antennas

In most cases in our life, there are many antennas distributed on the carrier platform to perform a variety of functions. The interaction between antennas and plane will change the antennas' performance a lot. Meanwhile, the coupling computation of antennas on platform can be hardly realized by experiment since the locations of them are changed. And also it is not possible to reinstall the antennas after they have already been installed on the platform. To solve the problem proposed above, one can use the precise electromagnetic computation technique to get the accurate layout scheme of antennas on the plane [1–3]. At present, there is a lot of commercial softwares which are capable of performing the layout simulation of antennas on the plane. However, the computation scale is not big in general. Only the model of hundreds MHz level can be calculated accurately. When the model with electrically large dimensions has to be simulated, the computation results will not be accurate because of the use of high frequency techniques, such as UTD and PO. Therefore, when the frequency is high, the large scale EM computation of the whole model becomes a great challenge to the engineers; HPC technique can be the best method to accelerate the calculation process [18–20]. In addition, the employment of MoM technique with higher order basis functions can guarantee the precision [1].

In order to validate the accuracy of this paper's method further, we compare the disturbed radiation patterns at 100 MHz obtained from this paper's method and RWG MoM method in the commercial software FEKO in the first part of this example. The model simulated is an aircraft with wire antennas 1 presented in Fig. 6, whose geometrical dimension is 36.1 m $\times$ 38 m $\times$ 7.8 m. The results of E

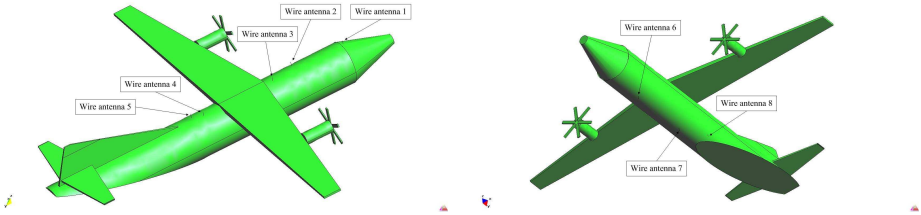

Figure 6. Model of an aircraft with 8 wire antennas.

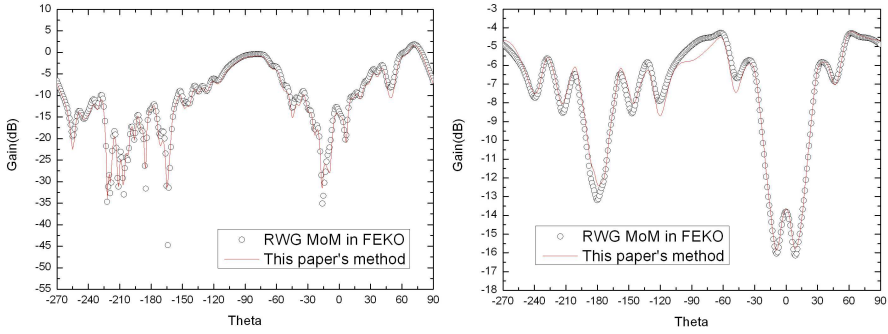

Figure 7. Comparison of E and H radiation patterns of antennas 1 (in dB). (a) Disturbed radiation patterns on E (YOZ) plane. (b) Disturbed radiation patterns on H (XOZ) plane.

Table 2. Number of unknowns.

Method	Number of unknowns
This paper's method	18456
RWG MoM in FEKO	29967

(YOZ plane) and H (XOZ plane) plane are illustrated in Fig. 7. And the respective numbers of unknowns are compared in Table 2. From the comparison, we can find that the results obtained are in good agreement so that the method in this paper is proved correct. And also the number of unknowns is reduced when higher-order basis is used, compared with the number of piecewise RWG basis functions.

In the second part of this example, a simulation of the same platform with a number of wire antennas has been conducted. The simulation frequency is 400 MHz. Thus, the corresponding electrical size is $48.1\lambda \times 50.7\lambda \times 10.4\lambda$, where λ is the wave length in free space. On the plane, there are 8 linear antennas mounted at different locations.

Table 3. Isolation parameters (dB).

	1	2	3	4	5	6	7	8
1		32	34	43	52	39	43	65
2			28	45	41	29	39	48
3				41	38	48	55	77
4					20	27	35	46
5						37	48	59
6							28	34
7								29
8								

All these antennas perform the functions of detection, early warning and control. The excitation port of each antenna is added 50 ohm load to realize the match so that maximum power output can be obtained.

After the calculation, we can obtain all the ports' (antennas') S parameters and substitute them into Eq. (15) to get the isolation parameters so as to determine the layout of the antennas. In Table 3, the isolation parameters between each two antennas are presented. The identifiers 1–8 in row one represent the antennas' number, so do the identifiers in column one. Coordinate (i, j) is considered as the location where "i" is row identifier and "j" column identifier. Thus the data with coordinate (i, j) represents the isolation parameter between antennas i and j. The results in the table are truncated to obtain the integer part of the digits, and the unit is dB. From the table, it can be found that each two antennas have a high isolation basically. Moreover, since the parameter of antennas' isolation is concerned with the radiation pattern, gain and distance, the isolation is higher when the antennas' distance is longer.

In the final part of this example, two situations are simulated: (1) calculation of the undisturbed radiation pattern of antenna 2; (2) calculation of the disturbed radiation pattern of antenna 2. Through the comparison of these two situations, the coupling effect of antennas on the radiation pattern is presented. The simulation frequency is also 400 MHz. And the respective models simulated are only antenna 2 on the plane in situation (1) and 8 antennas on the plane in situation (2). The comparison of the results is illustrated in Fig. 8.

From the comparison presented in Fig. 8, we can find the distortion of the radiation patterns, which is due to the coupling effect of antennas on the platform.

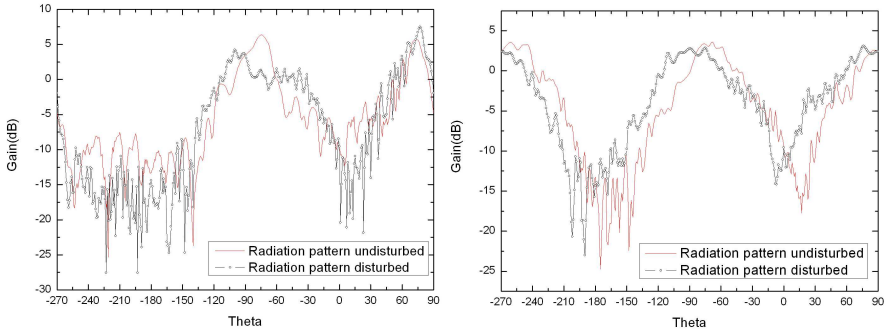

Figure 8. Comparison of E and H radiation patterns of antennas 2 (in dB): undisturbed situation versus disturbed situation. (a) Radiation patterns on E (YOZ) plane. (b) Radiation patterns on H (XOZ) plane.

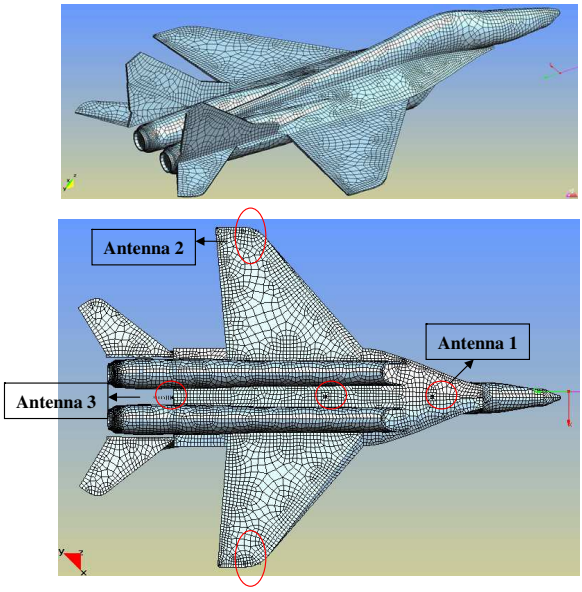

Figure 9. MIG29 model and its antennas' layout.

3.3. MIG 29 Plane with Two Patch Antennas and Three Yagi Antennas

In this example, a systematical EMC problem of Mig 29 plane has been simulated. The simulation frequency is 1 GHz so that the electrical dimensions of the aircraft are $57.7\lambda \times 40.7\lambda \times 12\lambda$. The plane is

an accurate curve model with air inlets, and there are five antennas mounted on it: two patch antennas and three Yagi antennas. These two patch antennas in the belly of the plane can be used as altimeters, while the three Yagi antennas mounted on the two wings and the tail are usually used to perform the functions of prediction and warning.

Figure 9 shows the plane model and the antennas mounted on it. The portion inside the circle is the location of the antenna.

Figure 10 illustrates the models of Yagi antenna and patch antenna mounted on this plane. From the picture, we can see that the Yagi antenna is composed of two reflector elements, a driven element and five director elements. And it is excited by a unit voltage source on the driven element; the patch antenna has dielectric base, patch and ground board. Coaxial line is used as the excitation.

Figure 11 presents the results of the induced current from antennas 1, 2, 3 and the 3D disturbed radiation pattern of them in dB. It is necessary to indicate that the results presented in Fig. 11 are the radiation patterns with the coupling effect among each antenna. We can see from the figure that all the antennas can obtain a relative good gain in their current locations. The maximum gain is 12.368 dB. It can be also found in Table 4 that the problem of huge computation amount and long calculation time as a result of the accurate computation has been greatly worked out with the help of large scale parallel computation scheme. The precise results can be obtained in less than three hours when 592 CPUs have been used in Shanghai Supercomputer Center (SSC), which provides an effective precise design method to the antennas' distribution on the electrically large platform.

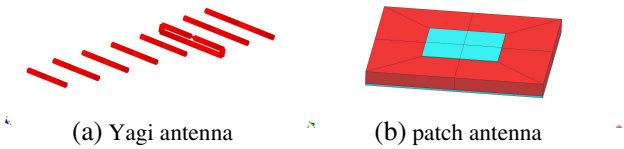

(a) Yagi antenna (b) patch antenna

Figure 10. Antenna model.

Table 4. Information of the accurate calculation of antennas' layout on MIG 29.

Benchmark's name	Number of Unknowns	Number of processes (Process grid)	Matrix Filling time (second)	Matrix Solving time (second)	Wall Clock time (second)
MIG29	181491	592 (16×37)	2187	7004	9594

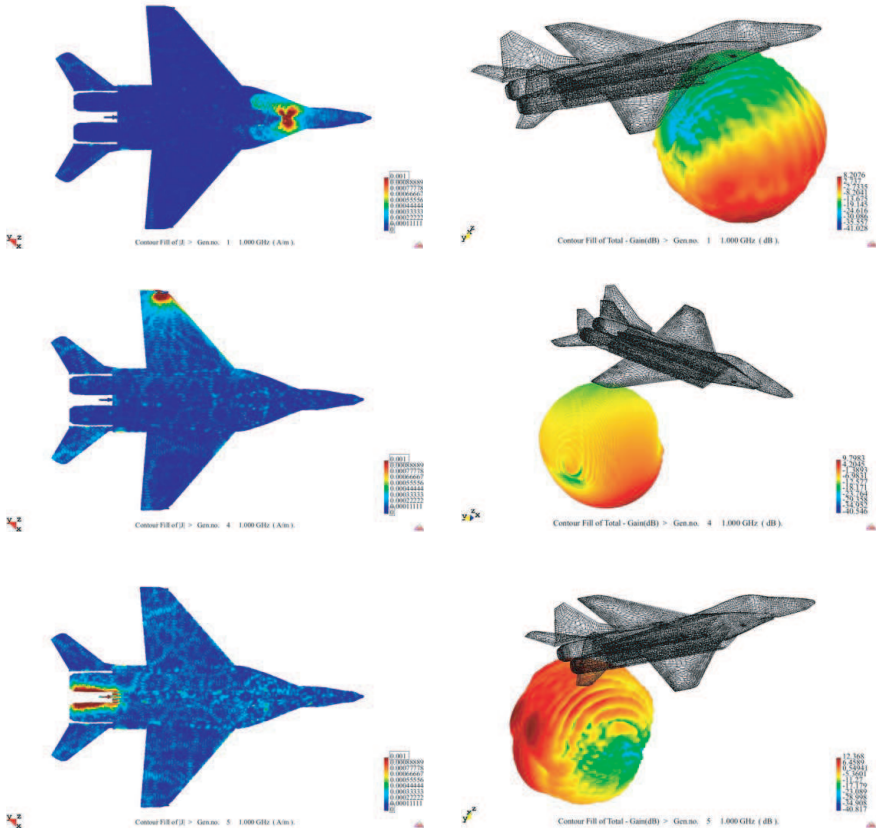

Figure 11. Induced current and 3D disturbed Radiation pattern (in dB) of antenna 1, 2 and 3.

4. CONCLUSION

In this paper, the parallel MoM technique with higher-order basis function is applied to solve the EMC problems of antenna mounted on large platform. By using this method, the radiation pattern and the isolation of antennas can be calculated simultaneously. Also the numerical examples show that this method is accurate and efficient to handle this kind of problem.

ACKNOWLEDGMENT

This work is partly supported by the Fundamental Research Funds for the Central Universities of China (JY10000902002, K50510020017),

the National Natural Science Foundation of China (61072019) and the Foundation of Science and Technology on Antenna and Microwave Laboratory (9140C070502110C0702). This work is also supported by Shanghai Supercomputer Center of China (SSC).

REFERENCES

1. Zhang, Y. and T. K. Sarkar, *Parallel solution of Integral Equation Based EM Problems in the Frequency Domain*, Wiley, Hoboken, NJ, 2009.
2. Harrington, R. F., *Field Computation by Moment Methods*, IEEE Series on Electromagnetic Waves, New York, IEEE, 1993.
3. Zhang, Y., *Parallel Computation in Electromagnetics*, Xidian University Press, Xi'an, China, 2006.
4. Rao, S. M., D. R. Wilton, and A. W. Glisson, "Electromagnetic scattering by surfaces of arbitrary shape," *IEEE Transactions on Antennas and Propagation*, Vol. 30, No. 5, 409–418, 1982.
5. Rao, S. M., C. C. Cha, R. L. Cravey, and D. L. Wilkes, "Electromagnetic scattering from arbitrary shaped conducting bodies coated with lossy materials of arbitrary thickness," *IEEE Transactions on Antennas and Propagation*, Vol. 39, No. 5, 627–631, May 1991.
6. Makarov, S., "MoM antenna simulations, with Matlab: RWG basis functions," *IEEE Magazine on Antennas and Propagation*, 100–107, 2001.
7. Sendur, I. K. and L. Gurel, "Solution of radiation problems using the fast multipole method," *IEEE International Symposium on Antennas and Propagation*, Vol. 1, 88–91, 1997.
8. Jakobus, U., J. van Tonder, and M. Schoeman, "Advanced EMC modeling by means of a parallel MLFMM and coupling with network theory," *IEEE International Symposium on Electromagnetic Compatibility*, 1–5, 2008.
9. Liu, Z.-L., J. Yang, and C.-H. Liang, "The hybrid higher-order MoM-UTD formulation for electromagnetic radiation problems," *19th International Symposium on Electromagnetic Compatibility*, 718–721, 2008.
10. Tap, K., T. Lertwiriyaprapa, P. H. Pathak, and K. Sertel, "A hybrid MoM-UTD analysis of the coupling between large multiple arrays on a large platform," *IEEE International Symposium on Antennas and Propagation*, Vol. 4A, 175–178, 2005.
11. Djordjevic, M. and B. M. Notaros, "Higher order hybrid method of moments — Physical optics modeling technique for radiation

and scattering from large perfectly conducting surfaces," *IEEE Transactions on Antennas and Propagation*, Vol. 53, No. 2, 800–813, Feb. 2005.

12. Chen, M., Y. Zhang, X.-W. Zhao, and C.-H. Liang, "Analysis of antenna around NURBS surface with hybrid MoM-PO technique," *IEEE Transactions on Antennas and Propagation*, Vol. 55, No. 2, 407–413, 2007.
13. Yan, Y., Y. Zhang, W. Zhao, X. Zhao, and T. K. Sarkar, "Analysis of antenna around target with dielectric coatings with hybrid MOM-PO technique," *IEEE International Symposium on Antennas and Propagation*, 3162–3165, 2011.
14. Jorgensen, E., P. Meincke, and O. Breinbjerg, "A hybrid PO-higher-order hierarchical MOM formulation using curvilinear geometry modeling," *IEEE International Symposium on Antennas and Propagation*, Vol. 4, 98–101, 2003.
15. Kolundzija, B. M. and B. D. Popovic, "Entire-domain galerkin method for analysis of metallic antennas and scatterers," *IEE Proceedings — H*, Vol. 140, No. 1, 1993.
16. Notaros, B. M., B. D. Popovic, and J. P. Weem, "Efficient large-domain MoM solutions to electrically large practical EM problems," *IEEE Transactions on Microwave Theory and Techniques*, Vol. 49, No. 1, 151–159, Jan. 2001.
17. Djordjevic, M. and B. M. Notaros, "Higher-order moment-method modeling of curved metallic antennas and scatterers," *IEEE International Symposium on Antennas and Propagation*, Vol. 4, 94–97, 2003.
18. Zhang, Y., M. Taylor, T. K. Sarkar, H. Moon, and M.-T. Yuan, "Solving large complex problems using a higher-order basis: Parallel in-core and out-of-core integral-equation solvers," *IEEE Antennas and Propag. Mag.*, Vol. 50, No. 4, 13–30, Aug. 2008.
19. Zhang, Y., M. Taylor, T. K. Sarkar, A. De, M.-T. Yuan, H. Moon, and C.-H. Liang, "Parallel in-core and out-of-core solution of electrically large problems using the RWG basis functions," *IEEE Antennas and Propag. Mag.*, Vol. 50, No. 5, 84–94, Oct. 2008.
20. Zhang, Y., T. K. Sarkar, M. Taylor, and H. Moon, "Solving MoM problems with million level unknowns using a parallel out-of-core solver on a high performance cluster," *IEEE Antennas and Propagation Soc. Int. Symp.*, Charleston, SC, USA, Jun. 1–5, 2009.
21. http://www.ssc.net.cn/